Numerical simulation of temperature and relative humidity in zero energy cool chamber

Liu Yanhua[1,2], Lyu Enli[1,2], Muhammad M. Rahman[2*], Wang Yu[1], Guo Jiaming[1], Zhang Jie[3]

(1. *College of Engineering, South China Agricultural University, Guangzhou 510642, China*;
2. *Department of Mechanical Engineering, University of South Florida, Tampa, FL 33620, USA*;
3. *Department of Civil and Environmental Engineering, University of South Florida, Tampa, FL 33620, USA*)

Abstract: Temperature and relative humidity are important parameters that can affect the storage of food in a zero energy cool chamber (ZECC). The distributions of average temperature and relative humidity are influenced by factors such as chamber size, water temperature, load weight and filler thickness. In this research, thermal environment analysis using numerical simulation of biological respiration was conducted for tomatoes stored in a ZECC. The ZECC was composed of inner and outer brick walls, filler (a mixture of sand and zeolite), water between the walls and a shading curtain. The results obtained from the numerical model were compared by setting different values for each factor. The following conclusions are drawn after comparison and analysis of results: (1) the distributions of average temperature and relative humidity are strongly related to the thickness of the filler – a thicker filler causes a lower temperature; (2) the water temperature in the filler exerts little influence on the average temperature and relative humidity; and (3) the lowest temperature and the highest relative humidity can be achieved with a chamber size of 0.6 m and a load weight of 30 kg. In addition, to validate the results of the numerical model, the simulation results are compared with experimental data, which show good agreement. It is confirmed that numerical simulation can be satisfactorily applied to predict the distribution of environmental parameters such as temperature and relative humidity in a cool chamber.

Keywords: zero energy cool chamber, numerical model, temperature, relative humidity
DOI: 10.3965/j.ijabe.20171003.3050

Citation: Liu Y H, Lyu E L, Rahman M M, Wang Y, Guo J M, Zhang J. Numerical simulation of temperature and relative humidity in zero energy cool chamber. Int J Agric & Biol Eng, 2017; 10(3): 185–193.

1 Introduction

A zero energy cool chamber (ZECC) for storing fruits and vegetables is an eco-friendly storage system developed from considerations of low cost and high energy efficiency. It does not need electrical energy and has a simple structure with outer and inner brick walls, a filler material between the brick walls, a storage space and a water supply system[1]. The filler is made of a mixture of sand and zeolite to maximize the retention of moisture within it. Inserting water into the filler can reduce the inside air temperature, based on the principle of a passive evaporative cooling mechanism. The liquid water molecules evaporate due to the humidity difference between the filler and the ambient air. During the process, the latent energy of evaporation for changing the physical state from liquid to vapor decreases the temperature of the filler and brick walls. As a result, the

Received date: 2016-12-01 **Accepted date:** 2017-03-20
Biographies: Liu Yanhua, Associate Professor, research interest: architectural engineering, Email: 24610597@qq.com; **Lyu Enli,** Professor, research interest: agricultural engineering, Email: enlilv@scau.edu.cn; **Wang Yu,** Lecturer, research interest: agricultural engineering, Email: yu-wang@scau.edu.cn; **Guo Jiaming,** Lecturer, research interest: agricultural engineering, Email: jmguo@scau.edu.cn; **Zhang Jie,** Lecturer, research interest: agricultural engineering, Email: 394303370@qq.com.
***Corresponding author: Muhammad M. Rahman,** Professor, research interest: architectural engineering. Department of Mechanical Engineering, University of South Florida, 4202 E Fowler Avenue, ENB118, Tampa, FL 33620, USA. Tel/Fax: (316) 978-3456, Email: Muhammad.Rahman@wichita.edu.

inside air temperature of the ZECC becomes lower, along with that of the products it contains. Hence, a ZECC can be used for storing fruit and vegetables when the ambient air is dry enough to generate an air temperature difference. It is useful for cooling and enhancing storage system efficiency in developing countries where energy efficiency may be critical[2], and it is beneficial to small farmers in rural areas[3]. Evaporative cooling is capable of inducing the processes of heat and mass transfer when water and air are the working fluids[4]. It reduces the temperature and increases the relative humidity of an enclosure, and has been extensively tested for enhancing the shelf-life of horticultural produce[4,5]. It is noted that temperature and relative humidity are important environmental parameters affecting the ripening process of fruits and their final quality in the storage chamber[6,7]. Singh and Satapathy[8] evaluated the performance of a ZECC, and found that the mean maximum temperature inside their cool chamber was about 5ºC and 6ºC lower than the ambient temperature during the summer and winter seasons, respectively. The relative humidity inside the cool chamber was 13.34% and 12.34% higher than the ambient humidity during the summer and winter months, respectively. The effect of adding water to a ZECC was studied by Ganesan et al.[9], who found that the shelf-life (three days at room temperature) could be enhanced to nine days with the addition of 100 liters of water per day. Anyanwu[10] showed that (cooler storage chamber temperature reduced from ambient air temperature varied over 0.1ºC-12ºC) and the evaporative cooler has prospects for short-term preservation of vegetables and fruits soon after harvest. Rajeswari et al.[11] conducted an experiment to assess the effect of pedicel retention and storage of Malta fruits in a ZECC, and found that weight loss and rotting were reduced to about half and that shelf-life could be extended to about 90 days, by storage of fruits in a ZECC. Weight loss for tomatoes stored at ambient temperature was 5.4%, but untreated fruits in a ZECC over the same period showed a 2.6% loss[12].

Although there are some related studies on the operation of a ZECC, how relevant parameters affect the cooling effectiveness and temperature distribution in a ZECC has rarely been investigated. Therefore, further studies are needed to evaluate the effect of parameter combinations in order to utilize them efficiently for various situations in the design and operation of a ZECC. A numerical model has been developed for predicting transient heat transfer in a pre-cooling operation[13]. It could calculate the cooling rates in beds of fruits and vegetables. Simplified heat transfer models have been developed for temperature prediction of domestic refrigerators, refrigerated display cabinets and refrigerated vehicles[14-16].

The increasing number of developments in numerical modeling in recent years has increased the possibility of using a low-cost effective method for modeling and simulation of airflow and heat transfer in a ZECC with fewer experiments. Three-dimensional (3D) models are generally considered to be complicated and time consuming. A two-dimensional (2D) model, which does not provide as much information as a 3D model, is still able to give valuable information about the air velocity, temperature and relative humidity profiles in a ZECC. By simplifying the geometry and conditions to two dimensions, solutions can be obtained in a reasonable amount of time. However, no thorough investigation of several parameters within a ZECC has been reported.

The main objective of this study is to simulate the 2D airflow and heat transfer in a ZECC using numerical modeling. The effects of several groups of parameters, such as chamber size, water temperature of filler, thickness of filler and load weight, on fluid flow and heat transfer in the ZECC are also explored. The detailed analysis of fluid flow, heat transfer and water vapor diffusion in the entire region will be a valuable contribution to the design and operation of a ZECC.

2 Mathematical model

The model of the ZECC is shown in Figure 1. The ZECC comprises inner and outer brick walls, a filler that is a mixture of sand and zeolite between the walls, a shading curtain and a storage space for tomatoes. A shading curtain (assuming a light transmittance of 40%) is set as the source of solar radiation, and can release heat flux to the surrounding area. The tomatoes can produce heat flux and water vapor flux through biological respiration. The evaporation of water modules absorbs heat, causing a reduction of the temperature in the ZECC. To predict the thermal environment, it is necessary to determine the air velocity, temperature and relative humidity in the ZECC. These can be computed by solving the coupled equations for the conservation of mass, momentum and energy of the airflow. The whole process is assumed to be a transient state of heat transfer, and the multi-component fluid composed of dry air and water vapor is treated as an incompressible flow of moist air.

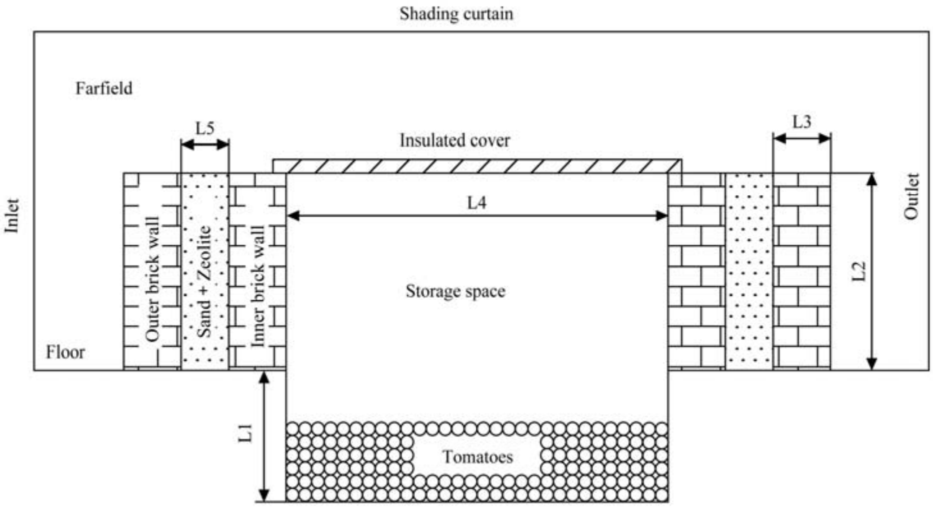

Note: L1 is 0.2 m; L2 is 0.3 m; L3 is 0.75 m; L4 is 0.4, 0.6 or 0.8 m; L5 is 0.025, 0. 075 or 0.125 m.

Figure 1 Sketch of Zero Energy Cool Chamber

Since airflow only exists in the far field, the governing equations for a far-field zone include the continuity equation, the incompressible Navier-Stokes equation and the heat transfer equation, while the governing equation for the rest of the zones is the heat transfer equation only.

The continuity equation is:

$$\nabla \cdot u=0 \tag{1}$$

where, u is the velocity vector, m/s.

The incompressible Navier-Stokes equation is:

$$\rho u \cdot \nabla u=-\nabla p+\mu \nabla^2 u+\rho g \beta (T-T_{ref}) \tag{2}$$

where, ρ is the density of air, 1.1967 kg/m^3; p is the pressure, Pa; μ is the viscosity of air, kg/m·s; g is the gravitational acceleration, m/s^2; β is the thermal expansion coefficient, 0.003932 K^{-1}; T is the temperature, °C; T_{ref} is the reference temperature, °C.

The general heat transfer equation can be expressed as:

$$\rho c_p u \cdot \nabla T = k \nabla^2 T + S \tag{3}$$

where, c_p is the specific heat of air, kJ/kg·K; k is the thermal conductivity of air, W/m·K; and S is the heat source of the tomatoes, W/m³.

To accurately define the problem, appropriate boundary conditions are required at every boundary segment of the computational domain. For the continuity Equation (1) and the momentum Equation (2), boundary conditions are applied as follows: a prescribed velocity for the inlet and zero velocity for solid surfaces. For the energy Equation (3), a constant temperature condition is used for the inlet, there is a constant heat flux for the biological respiration of the tomatoes, there is a variable heat flux for the water evaporation process and there is solar radiation from the shading curtain.

The solution is obtained from solving Equations (1) to (3), with their associated boundary conditions, and the following five primary parameters are specified: two velocity components, pressure, temperature and water vapor concentration. The relative humidity can be calculated using the following procedure as recommended by ASHRAE[19]:

$$\varphi = \frac{p_w}{p_{ws}} \tag{4}$$

where,

$$p_w = \frac{(101325 + p)m_1}{0.62198 + 0.37802 m_1} \tag{5}$$

$$p_{ws} = 1000\exp[-5.800\times10^{3}(T+273.15)^{-1} - 5.516] - 0.04864(T+273.15) + 4.176\times10^{-5}(T+273.15)^{2} - 1.445\times10^{-8}(T+273.15)^{3} + 6.546\ln(T+273.15)] \quad (6)$$

where, φ is the relative humidity; p_w is the partial pressure of water vapor in moist air, Pa; p_{ws} is the pressure of saturated water, Pa; and m_1 is the concentration (mass ratio) of water vapor (kg/kg of moist air).

3 Numerical solution

The essential dimensions are denoted in general forms as L1 to L5 in Figure 1. L1 to L3 are fixed numerical values as follows: L1=0.2 m, L2=0.3 m and L3=0.075 m. They are chosen based on the real typical dimensions of corresponding objects. The numerical values of L4, L5, load weight and temperature of water in the mixture for each simulation are given in Table 1.

Table 1 Simulation cases

Simulation case #	Objects	L4 /m	L5 /m	Load weight /kg	Water temperature /°C
1	Air temperature, humidity and velocity	0.6	0.075	30	20
2	Air temperature and humidity	0.6	0.025	30	20
3	Air temperature and humidity	0.6	0.125	30	20
4	Air temperature and humidity	0.4	0.075	30	20
5	Air temperature and humidity	0.8	0.075	30	20
6	Air temperature and humidity	0.6	0.125	15	20
7	Air temperature and humidity	0.6	0.125	60	20
8	Air temperature and humidity	0.6	0.075	30	30
9	Air temperature and humidity	0.6	0.075	30	10

The water molecules in the filler absorb heat and evaporate, which causes the temperatures of the filler and brick walls to decrease. The air temperature inside the ZECC, along with that of the tomatoes, also decreases due to heat transfer. During this process, the thickness of the filler, the water temperature in the filler, the size of the storage space and the load weight may be factors that affect heat transfer. A typical set of these factors is provided by Islam et al.[12]: thickness of filler 0.075 m, water temperature 25ºC, size of storage space 0.6 m and load weight 30 kg. To investigate how these factors affect heat transfer, another two sets of test values for each factor are considered in this study. These are: filler thickness: 0.025 m and 0.125 m; water temperature: 10ºC and 30ºC; size of storage space: 0.4 m and 0.8 m; and load weight: 15 kg and 60 kg. In total, nine simulation cases are performed.

In order to save computational time, the two hours from 15:00 to 17:00 are chosen for the transient state simulation. The simulation results on the changes of temperature and relative humidity can be verified by comparison with the experimental results of Islam et al.[12] The resulting values of water temperature, chamber size, filler thickness and weight load are compared at the time 17:00.

The equation for the solar radiation source set by the shading curtain at the time interval from 15:00 to 17:00 is given by:

$$q=\mathrm{a}t+\mathrm{b} \quad (7)$$

where, q is the heat flux, W/m^2; t is the time, s; a=–1.668×10^{-2} W/m^2 s; and b=240 W/m^2.

The heat transfer equations for the evaporation of water molecules in the filler are:

$$q_{wv} = k_w(p_w - p_{ws}) \quad (8)$$

$$q_{hv} = L_v q_{wv} \quad (9)$$

where, q_{wv} is the mass flux for water evaporation, kg/s; k_w is the mass flux coefficient of water evaporation, kg/(Pa s); q_{hv} is the heat flux for water evaporation, W; and L_v is the latent heat of water evaporation (2257 kJ/kg).

Details of the boundary conditions are given in Table 2. The properties of air are taken at a reference temperature of T_{ref} =22°C as follows: ρ=1.1967 kg/m^3; μ=1.8273×10^{-5} kg/m·s; c_p=1.0043 kJ/kg·K; k = 0.025776 W/m·K; β, the thermal expansion coefficient, 0.003932 1/K; and D, the diffusion coefficient, 2.5449×10^{-5} m^2/s[17]. The properties of the filler are as follows: ρ=3606 kg/m^3, c_p=912 kJ/kg·K and k=0.3993 W/m·K (calculated from the ratio of sand to zeolite). The properties of the tomatoes are: ρ=1000 kg/m^3, c_p=3680 kJ/kg·K and k=0.47 W/m·K[20]. The heat and mass of respiration of the tomatoes are estimated using IIR data[18]. q_{hr} is the heat of respiration of the product, W/kg.

Initial conditions are essential for the simulation of the transient state. The initial temperature and relative humidity for the far field and storage space, the solar radiation, the inlet velocity and the water temperature are given by Islam et al.[12] However, the other initial conditions of the brick walls, filler and tomatoes are still unknown. Thus, an additional simulation is conducted to determine the other parameters for the initial conditions, which are listed in Table 3.

Table 2 Boundary conditions

Entity	Velocity/m·s^{-1}	Temperature/°C	Water vapor/kg·s^{-1}
Inlet	u_x=0.5	T=37	φ=60%
Outer brick wall	u_x= u_y=0	q =0	q_w=0
Inner brick wall	u_x= u_y=0	q =0	q_w=0
Shading curtain	u_x= u_y=0	Eq.(7)	q_w=0
Filler	u_x= u_y=0	Equation (9)	Equation (8)
Tomatoes	u_x= u_y=0	q_{hr} =0.0154	q_{wr}=3.1453E-5
Storage space	u_x= u_y=0	q=0	q_w=0
Insulated cover	u_x= u_y=0	q=0	q_w=0

Table 3 Initial conditions

Entity	Temperature/°C	Water vapor/kg·s^{-1}
Inlet	T=37	60%
Outer brick wall	T=23.5	
Filler	See Table 1	
Inner brick wall	T=22.9	
Tomatoes	T=23.2	82%
Storage space	T=23.1	82%

4 Results and discussion

Figure 2 shows the distributions of air velocity, temperature and relative humidity for Simulation 1. According to the speed distribution in Figure 2a, the outside airflow enters the inlet through the far field at a uniform speed (0.5 m/s). Due to blocking by the outer brick wall, the flow goes through the gap between the shading curtain and the insulated cover at a higher speed (maximum speed is 2.8 m/s). There is a slight circulation in the region between the right outer brick wall and the outlet, caused by a small airflow separated from the main airflow. In the storage space, the inside airflow speed in the storage space is relatively low, especially in the area of the tomatoes (near to 0 m/s). The outside airflow is mainly forced convection by the inlet velocity, and the inside airflow is dominated by natural convection due to the temperature difference between the inner brick walls and the inner air.

Figure 2b presents the temperature distribution for a typical case (Simulation 1). The far-field region has the same temperature as the inlet air, thus, the outside airflow is strong enough to maintain the heat transfer between the air and the surfaces of the ZECC. The water molecules in the filler evaporate and take heat away, making the filler the cold source of the ZECC. The temperature of the outer brick walls is higher than that of the inner ones, because the outer bricks receive the heat transferred from the high temperature outside in the ambient air. Meanwhile, the temperature of the left-hand bricks and filler is higher than the right-hand ones, as the airflow speed of the left-hand outer is higher than that of the right-hand one. A colder storage space is constructed with an average temperature of 23.65°C including the tomato area, which is 13.35°C lower than the outside air.

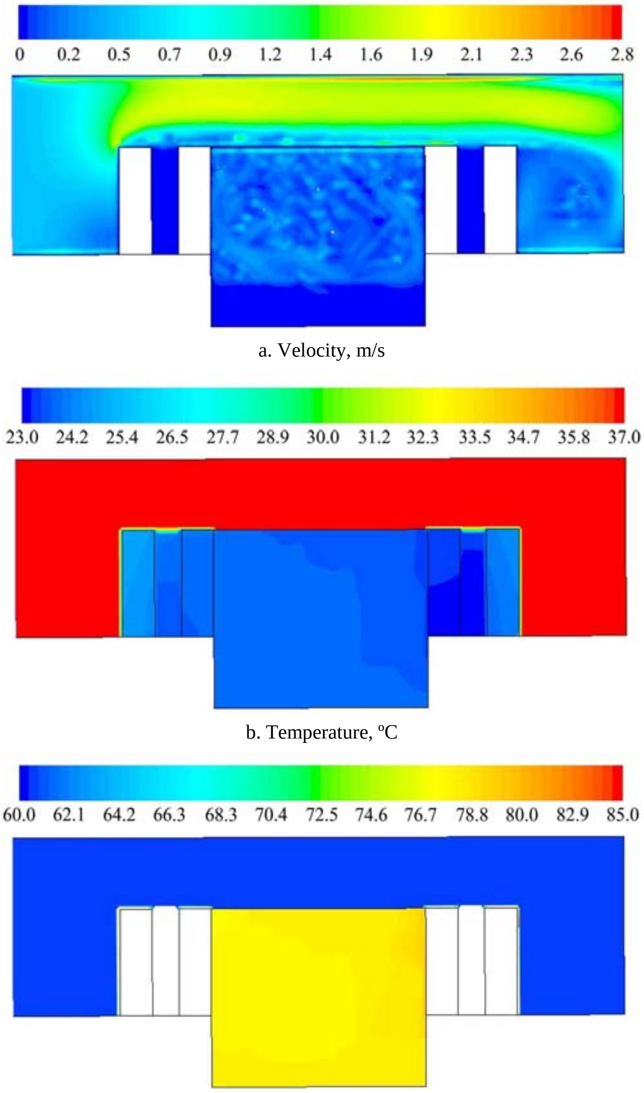

a. Velocity, m/s

b. Temperature, ºC

c. Relative humidity, %

Figure 2 Distribution of velocity, temperature and relative humidity for Simulation 1

Figure 2c shows the relative humidity distribution for Simulation 1. The evaporation of water molecules in the filler forced by the outside unsaturated air increases the relative humidity of the air above the filler, and the water vapor is taken away rapidly by the high-speed outside airflow. Therefore, the relative humidity at the far field is the same as at the inlet. Relative humidity is a parameter related to absolute pressure, water vapor concentration and temperature. In the storage space, the gage pressure is too small to affect the absolute pressure. Meanwhile, the water vapor from the tomatoes results in a very small flux. Thus, the relative humidity distribution is mainly dependent on the temperature distribution, which can explain the similar contours of their distributions. The average humidity in the storage space is 78.4%, which is 18.4% higher than that of the outside air.

The results from Simulations 2 and 3 show some different distributions for the temperature and relative humidity with respect to different thickness of filler. To facilitate analysis of the thermal environment in the storage space, the vertical distributions of the temperature and relative humidity are taken into account. At each different height, average temperature and relative humidity are observed over the whole width of the storage space.

Figure 3 compares the vertical distributions of temperature and relative humidity for three cases of different thickness of filler. In Figure 3a, the average temperature shows a high correlation with the thickness of filler: a thicker filler leads to a lower temperature. In the tomato area, the average temperature for the filler with thickness of 0.125 m (Simulation 3) was 21.9°C, which was 1.8°C lower than that of the other thickness fillers. A typical case shows a uniform vertical distribution of temperature in a narrow range of 23.0°C-23.7°C. The temperatures of the filler with 0.025 m thickness (Simulation 2) and the filler with 0.125 m thickness (Simulation 3) showed uniform distributions in the tomato area but varied significantly above the tomato area. Since the temperature in the tomato area is important for storage, the filler with 0.125 m thickness (Simulation 3) showed the best performance in this aspect.

Figure 3b shows the comparison of the vertical distributions of average relative humidity in the cases of three different thickness fillers. The distribution of relative humidity is consistent with that of the temperature, and it can be seen that a higher temperature leads to a lower relative humidity. The typical case had the most uniform distribution of relative humidity, ranging from 77.9% to 78.1%. For the fillers with thickness of 0.025 m and 0.125 m, there were significant changes of relative humidity, ranging from 69.1% to 78.2% and 80.8% to 86.9%, respectively. Relative humidity was higher in the tomato area and lower at a height closer to the insulated cover.

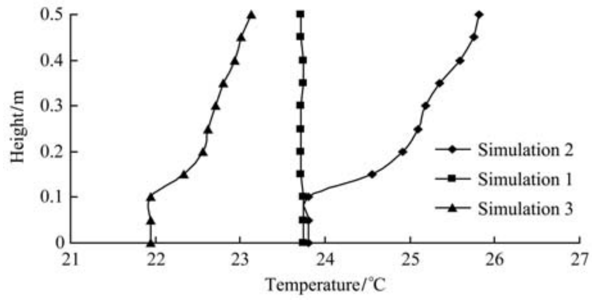

a. Average temperature

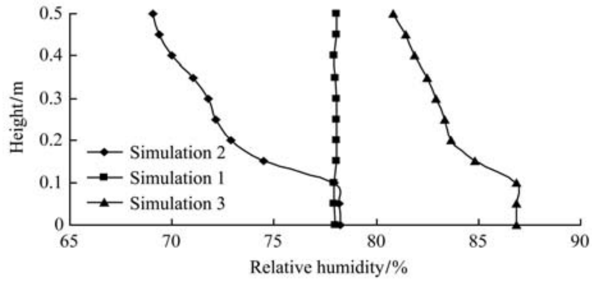

b. Average relative humidity

Figure 3 Vertical distributions of average temperature and relative humidity in the cases of different thickness fillers

Figure 4 compares the vertical distributions of average temperature and relative humidity for different chamber sizes. All three cases have the same load weight, but the height of the tomato area is different for the three different chamber sizes. In Figure 4a, the typical case shows the most uniform and lowest temperature distribution. However, the chamber sizes of 0.4 m (Simulation 4) and 0.8 m (Simulation 5) show obvious changes at different heights. In the tomato area, the temperature of Simulation 5 is 25.8°C, which is 2.0°C and 1.5°C higher than that in Simulation 1 and Simulation 4, respectively.

The vertical distribution of the average relative humidity for different chamber sizes is presented in Figure 4b. The typical case shows the most uniform relative humidity distribution, while for the cases with sizes of 0.4 m and 0.8 m, the relative humidity distribution changes are in the ranges 72.8% to 76.1% and 68.9% to 73.5%, respectively. The average relative humidity of the cases from high to low is the case with the size of 0.6 m, 0.4 m and 0.8 m.

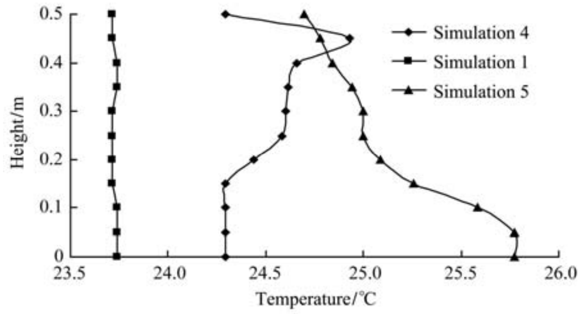

a. Average temperature

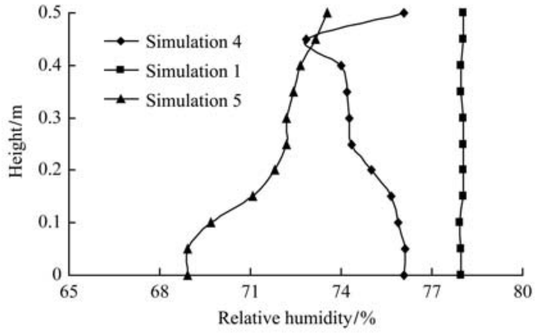

b. Average relative humidity

Figure 4 Vertical distributions of average temperature and relative humidity for different chamber sizes

A comparison among the three different load weight cases for the vertical distributions of temperature and relative humidity is shown in Figure 5a. All three cases show uniform vertical distributions of temperature and relative humidity. A typical case with a 30 kg load weight has the lowest average temperature (23.7°C). The average temperature for the case with a lower load weight (15 kg in Simulation 6) is 1.2°C higher than that for the typical case, and the case with a heavier load (60 kg in Simulation 7) has the highest average temperature (25.8°C).

Figure 5b shows the vertical distribution of relative humidity for different load weights. Similarly, the relative humidity distribution shows a strong dependency on the temperature distribution, and the shapes of the distribution curves for each parameter are also very similar. Moreover, the relative humidity for the typical case is 5.5%, which is 9.3% higher than the cases with load weights of 15 kg and 60 kg, respectively.

Figures 6a and 6b show the temperature and relative humidity distributions under different water temperatures of filler. In Figure 6a, the water temperatures show little influence on the average temperature of the storage space, and the three cases have the same average temperature zone (23.71°C-23.73°C), which are distributed uniformly. According to the plot of vertical relative humidity distribution in Figure 6b, the water temperatures still have little effect on the average relative humidity of the storage space, and the average relative humidity of the three cases ranges from 77.9% to 78.3%.

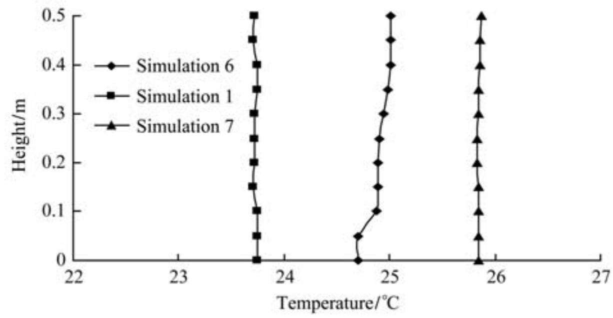

a. Average temperature

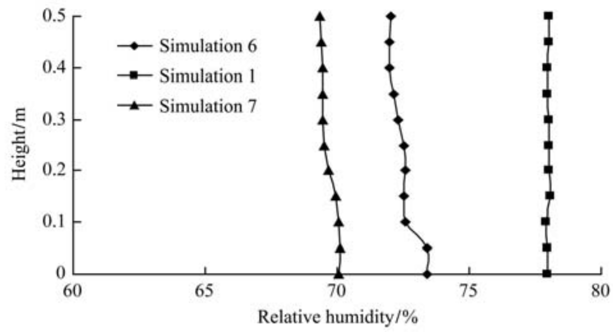

b. Average relative humidity

Figure 5 Vertical distributions of average temperature and relative humidity for different load weights

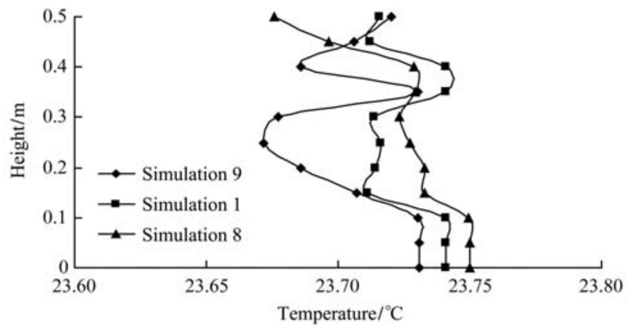

a. Average temperature

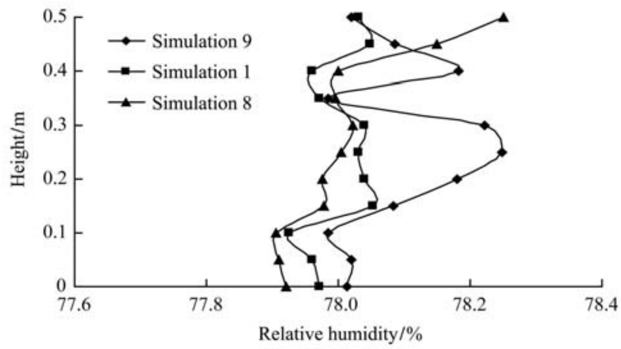

b. Average relative humidity

Figure 6 Vertical distributions of average temperature and relative humidity for different water temperatures

Figures 7a and 7b compare the results of a typical case and experimental data given by Islam et al.[12] The numerical simulation and experimental results show good agreement. The maximum differences of temperature and relative humidity between numerical simulation and experimental data are 0.7°C and 1.9%, respectively.

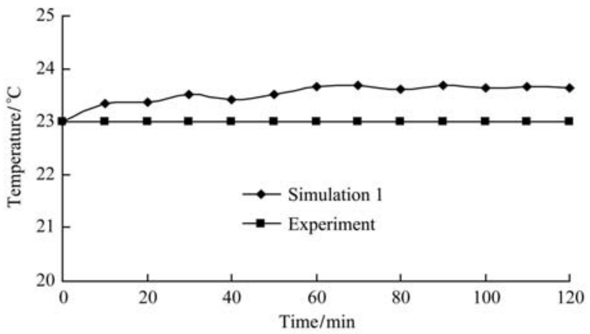

a. Average temperature

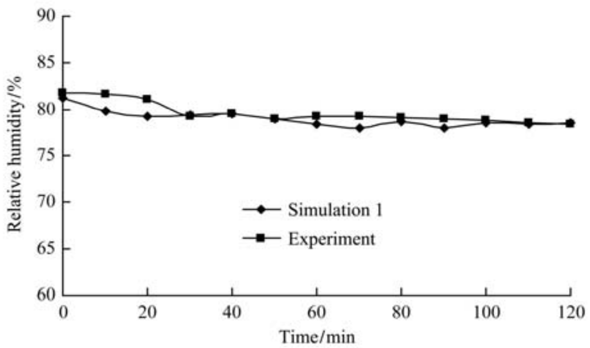

b. Average relative humidity

Figure 7 Comparison between simulation and experimental data

5 Conclusions

The results from the numerical simulations provide an insightful understanding into fluid flow and heat transfer in a ZECC. The evaporation of water molecules in the filler reduces air temperature in the chamber, which removes calorific energy from fresh produce, and generates a significant temperature difference for storing fruit and vegetables. The distributions of average temperature and relative humidity for the storage space in chambers of sizes 0.4 m, 0.6 m or 0.8 m in this study showed a high correlation with the thickness of filler: a thicker filler, with more evaporation of water, leads to a lower air temperature. The water temperatures in the filler exert little influence on the average temperature and relative humidity in the ZECC. The lowest temperature and highest relative humidity in the chamber can be achieved when the chamber size is 0.6 m, the filler size is 0.075 m and the load weight is 30 kg.

Moreover, numerical simulation results are in agreement with experimental data, which demonstrates that the numerical simulation can be effectively applied for predicting the distribution of velocity, temperature and relative humidity in a ZECC.

Acknowledgments

The authors acknowledge the financial support from the China Scholarship Council, the National Science and Technology Support Program of China (2015BAD18B0301), the Science and Technology Plan Projects of Guangdong - Postharvest Quality Value-added Storage and Energy Saving Technology and Equipment for Litchi and Longan (20170206), and the Strong and Innovation Projects of South China Agricultural University - Key Techniques on Energy Saving and Fresh-keeping of Litchi Storage (cold energy accumulation or CA storage) (2017).

[References]

[1] Islam M P, Morimoto T, Hatou K. Dynamic optimization of inside temperature of Zero Energy Cool Chamber for storing fruits and vegetables using networks and genetic algorithms. Computers and Electronics in Agriculture, 2013; 95: 98–107.

[2] Lal Basediya A, Samuel D V K, Beera V. Evaporative cooling system for storage of fruits and vegetables – a review. Journal of Food Science and Technology, 2013; 50(3): 429–442.

[3] Dadhich S M, Dadhich H, Verma R C. Comparative study on storage of fruits and vegetables in evaporative cool chamber and in ambient. International Journal of Food Engineering, 2008; 4(1): 1–11.

[4] Camargo J R. Evaporative cooling: water for thermal comfort. An Interdisciplinary of Journal Applied Science, 2007; 3(2): 51–61.

[5] Odesola I F, Onyebuchi O. A review of porous evaporative cooling for the preservation of fruits and vegetables. Pacific Journal of Science and Technology, 2009; 10(2): 935–941.

[6] Roy S K, Pal R K. A low cost zero energy cool chamber for short term storage of mango. Acta Horticulturae, 1991; 291: 519–524.

[7] Elazar R. Postharvest physiology, pathology and handling of fresh commodities. Lecture Notes. Department of Market Research. Ministry of Agriculture and Rural Development, Israel, 2004.

[8] Singh R K P, Satapathy K K. Performance evaluation of zero energy cool chamber in hilly region. Agricultural Engineering Today, 2006; 30(5-6): 47–56.

[9] Ganesan M, Balasubramanisan K, Bhavani R V. Effect of water on the shelf-life of brinjal in zero-energy cool chamber. Journal of the Indian Institute of Science, 2004; 84: 1–7.

[10] Anyanwu E E. Design and measured performance of a porous evaporative cooler for preservation of fruits and vegetables. Energy Conversion and Management, 2004; 45(13&14): 2187–2195.

[11] Rajeswari D, Nautiyal M C, sharma S K. Effect of pedicel retention and zero energy cool chamber on storage behavior of Malta fruits. International Journal of Agriculture Sciences, 2011; 3(2): 78–81.

[12] Islam M P, Morimoto T, Hatou K. Storage behavior of tomato inside a zero energy cool chamber. Agricultural Engineering International: CIGR Journal, 2012; 14(4): 209–217.

[13] Baird C D, Gaffney J J. A numerical procedure for calculating heat transfer in bulk loads of fruits or vegetables. ASHREAE Transactions, 1976; 82: 525–535.

[14] Laguerre O, Flick D. Temperature prediction in domestic refrigerators: Deterministic and stochastic approaches. International Journal of Refrigeration, 2010; 33: 41–51.

[15] Laguerre O, Derens E, Flick D. Temperature prediction in a refrigeration display cabinet: Deterministic and stochastic approaches. Electronic Journal of Applied Statistical Analysis, 2011; 4(2): 191 – 202.

[16] Hoang M H, Laguerre O, Moureh J, Flick D. Heat transfer modeling in a ventilated cavity loaded with food product: Application to a refrigerated vehicle. Journal of Food Engineering, 2012; 113: 389–398.

[17] Ho S H, Rosario L, Rahman M M. Thermal comfort enhancement by using a ceiling fan. Applied Thermal Engineering, 2009; 29: 1648–1656.

[18] IIR, International Institute of Refrigeration. Recommended conditions for cold storage of perishable products, 1971.

[19] ASHRAE handbook of fundamentals. Atlanta: American society of heating, refrigerating and air conditioning engineers, Inc. 2013.

[20] Lyu E L, Lu H Z, Yang Z, Liu C C, Guo J M. Pressure drop characteristics in forced-air pre-cooling of tomatoes. Transactions of the CSAE, 2010; 26(7): 341–345. (in Chinese)